

Table 1 Calculated values of  $\sigma_n$ 

$l$	$V$	$\sigma_n^a$
0.25	0.07	$<10^{-3}$
	0.10	0.001
	0.20	0.003
	0.50	0.015
	1.0	0.038
0.50	0.07	0.002
	0.10	0.003
	0.20	0.013
	0.50	0.060
	1.0	0.139
0.75	0.07	0.003
	0.10	0.007
	0.20	0.025
	0.50	0.117
	1.0	0.253
1.0	0.07	0.005
	0.10	0.010
	0.20	0.038
	0.50	0.171
	1.0	0.353
1.2	0.07	0.006
	0.10	0.012
	0.20	0.045
	0.50	0.203
	1.0	0.411
(2) <sup>1/2</sup>	0.07	0.007
	0.10	0.013
	0.20	0.049
	0.50	0.223
	1.0	0.450

<sup>a</sup> For  $V < 0.01$  the calculated value of  $\sigma_n$  was  $<10^{-3}$  for all  $l$ .

surface is assumed uniform in the  $z$  direction, it takes the form of an array of rigid cylinders of diameter  $d_s$  with their axes lying parallel to the  $z$  axis a distance  $L$  apart. Thus, the region unavailable to the centers of the gas molecules is bound by a series of segments of infinite parallel cylinders of diameter  $d = \frac{1}{2}(d_s + d_s)$ . The plane of the "macroscopic" surface  $y = 0$  is that tangent to the cylindrical segments, so the centers of the surface atoms lie in the plane  $y = -d$ . Because the collisions are impulsive and the surface is rigid, the collision function  $\theta'(x, \theta)$  can be determined analytically from the geometry of the collision trajectory for given values of the size ratio  $l = L/d$ .

Values of  $\sigma_n$  were calculated by numerical integration of Eq. (7) on an IBM 7040/7094 computer. The results are given in Table 1 for thirty pairs of values for  $l$  and  $V$ . In addition to the results given in Table 1, calculations of  $\sigma_n$  were also done for low velocities,  $V \leq 0.01$ . The values found, however, were all below  $10^{-3}$ , so that the surface model used here indicates that essentially no normal momentum is transferred from the gas to the surface when the dimensionless gas velocity is below 0.01. In fact, inspection of Table 1 shows that normal momentum transport is quite low, even for microscopically rough surfaces ( $l$  large), for gas velocities below  $V = 0.5$ . However, for high gas velocities, this is not the case. A value of  $V = 1$  corresponds to a gas velocity of about 1000 fps at 300°K. At this high gas velocity there is a significant amount of normal momentum transfer;  $\sigma_n = 0.25 - 0.41$  in the range of  $l = 0.75 - 1.2$  typical of most surfaces.

Care should be taken in giving too much quantitative significance to the above results. In contrast with the case of tangential momentum transport, the applicability of an infinitely massive, monocrystalline surface model to normal momentum transport is not clear. As discussed previously, however, the effect of assuming immobile surface atoms is to lower  $\sigma_n$ . Similarly, the assumptions of an ideal two-dimensional crystalline surface and of impulsive interactions also decrease  $\sigma_n$ . These factors strongly suggest that the calculated values of  $\sigma_n$  reported here represent a lower bound.

Consequently, the results of this study imply that, for high-speed gas flows, a significant fraction of the incident normal momentum will be transferred to any solid surfaces as a result of gas-surface collisions.

### References

<sup>1</sup> Notter, R. H., Kaku, Y. J., and Sather, N. F., "A Molecular Model for Tangential Momentum Accommodation," *ATAA Journal*, Vol. 8, No. 11, Nov. 1970, pp. 2064-2066.

<sup>2</sup> McClure, J. D., "Atomic and Molecular Scattering from Solids. II. Comparison of Classical Scattering Models in Relation to Experiment," *Journal of Chemical Physics*, Vol. 51, No. 5, Sept. 1969, pp. 1687-1700.

## Laminar Boundary Layers with Large Wall Heating and Flow Acceleration

L. H. BACK\*

*Jet Propulsion Laboratory, California Institute of Technology, Pasadena, Calif.*

### I. Introduction

THIS Note is concerned with evaluating the simultaneous effects of wall heating and acceleration on the structure of laminar boundary layers. Earlier similarity solutions for perfect gases with viscosity proportional to temperature and Prandtl number of unity by Cohen and Reshotko<sup>1</sup> indicated a beneficial increase in the heat-transfer parameter  $G_w'$ , to which the heat flux is related, as the heating parameter  $g_w$ , the ratio of wall to total enthalpy, was increased when flow acceleration occurred. Their calculations were carried out for values of  $g_w$  and  $\beta$ , a parameter descriptive of the free-stream velocity variation, up to 2. A range of  $g_w$  and  $\beta$  up to 5 is considered in this investigation so that predictions will be available for larger wall heating (e.g., in channel flows in nuclear rockets and in resistojets) and for larger freestream velocity variations (e.g., see Ref. 2 for the magnitude of  $\beta$  found in internal flows). Investigations of the effect of relatively large values of the heating parameter have been carried out for laminar boundary layers, but they apply to flows with no freestream velocity variation ( $\beta = 0$ ) for  $g_w$  from 1 to 10 (Ref. 3), for  $g_w$  from 1 to 6 in which compressibility effects are included,<sup>4</sup> or at a stagnation point with the effect of mass transfer included ( $\beta = \frac{1}{2}$ , axisymmetric body,  $\beta = 1$ , two-dimensional body) for  $g_w$  from 1 to infinity.<sup>5</sup>

### II. Analysis

The coupled, transformed, laminar boundary-layer equations that are solved numerically are as follows:

$$f''' + ff'' + \beta[G(1 - g_w) + g_w - (f')^2] = 0 \quad (1)$$

$$G'' + fG' = 0 \quad (2)$$

The reader is referred to Ref. 6 for a description of the various quantities in Eqs. (1) and (2), and other quantities that appear herein. The application of the solutions to actual flows with variable  $\beta$  and more realistic property variation is discussed later.

Received October 16, 1970; revision received February 1, 1970. This paper presents the results of one phase of research carried out in the Propulsion Research and Advanced Concepts Section of the Jet Propulsion Laboratory, under Contract NAS 7-100, sponsored by NASA. The author expresses his gratitude to P. Breckheimer of JPL, who carried out the numerical calculations.

\* Member Technical Staff. Associate Fellow AIAA.

### III. Results

The surface heat flux and shear stress are given in terms of the slopes of the profiles at the surface in the transformed plane  $G_w'$  and  $f_w''$ , as follows:

$$St = \frac{q}{(H_w - H_{10})\rho_e u_e} = \frac{1}{(Re_{\bar{x}})^{1/2}} \frac{G_w'}{(2)^{1/2}} \quad (3)$$

$$\frac{c_f}{2} = \frac{\tau}{\rho_e u_e^2} = \frac{1}{(Re_{\bar{x}})^{1/2}} \frac{f_w''}{(2)^{1/2}} \quad (4)$$

Both the parameters  $G_w'$  and  $f_w''$  shown in Fig. 1 increase with wall heating and flow acceleration. This trend does indicate an advantage of heating in an acceleration region. Of course, the heat flux also depends on other quantities [Eq. (3)] and therefore would increase as the mass flux increases in an accelerated, subsonic flow. The wall friction parameter  $f_w''$  increases more than  $G_w'$  does with heating and acceleration, however, so that the Reynolds analogy factor  $St/(c_f/2) = G_w'/f_w''$ , which is considerably reduced by acceleration (Fig. 1), decreases even more with heating. The correspondingly higher wall friction than heat transfer does indicate limitations on those applications where frictional effects are important. However, in many accelerating flows of practical interest, the shear forces that retard the flow are usually small compared to the pressure forces that accelerate the flow, and therefore frictional effects are not of much consequence.

The effects of wall heating, acceleration, and flow speed on the velocity and total enthalpy profiles in the physical  $x, y$  plane are shown in Fig. 2 in terms of the coordinate  $\zeta$ . In the coordinate  $\zeta$  the profiles depend upon the flow speed parameter  $S$  besides the heating and acceleration parameters. With wall heating, both the velocity and total enthalpy profiles become less steep near the wall, and velocities in the boundary layer exceed the freestream value. This latter condition, referred to as velocity overshoot, occurs in accelerated boundary layers with wall heating apparently because the external pressure gradient  $dp/dx$  impressed on the boundary layer is hardly balanced by shear forces in the outer part of the boundary layer since the velocity gradient  $\partial u/\partial y$  there is diminished. In fact, beyond the peak velocity, the shear force acts to accelerate the flow. Consequently, local acceleration  $\rho u \partial u/\partial x$  can occur and lead to velocity overshoot because of wall heating since there is a deficit in gas density in this region relative to the freestream.<sup>1</sup> Both the velocity and thermal layers increase in thickness with wall heating. The effect of acceleration is to increase the slope of the profiles near the wall and to increase the amount of velocity overshoot. The influence of flow speed (compressibility) on the profiles is to thicken the velocity and thermal boundary layers owing to viscous dissipation.

For the values of the heating, acceleration, and flow speed parameters investigated, the velocity profiles in an acceleration region do not have an inflection point in the region near the wall where the velocity increases as they do have in a nonaccelerating flow over a heated wall—Fig. 2b,  $\beta = 0$ , and Ref. 3. Hence, the boundary layer would be more stable to small disturbances.

Additional information on various quantities of interest is given in Table 1. Of note are the rather large increases in displacement  $\delta^*$ , velocity  $\delta$ , and thermal  $\delta_t$  boundary-layer thicknesses with wall heating and flow speed, although flow acceleration reduces these thicknesses. Negative values of the momentum thickness  $\theta$  occur because of the magnitude of velocity overshoot with larger wall heating and flow acceleration.

To utilize the similarity solutions to predict heat transfer, it is suggested that the following relation be used since it contains a Prandtl number correction and accordingly a more appropriate driving potential between wall and adiabatic

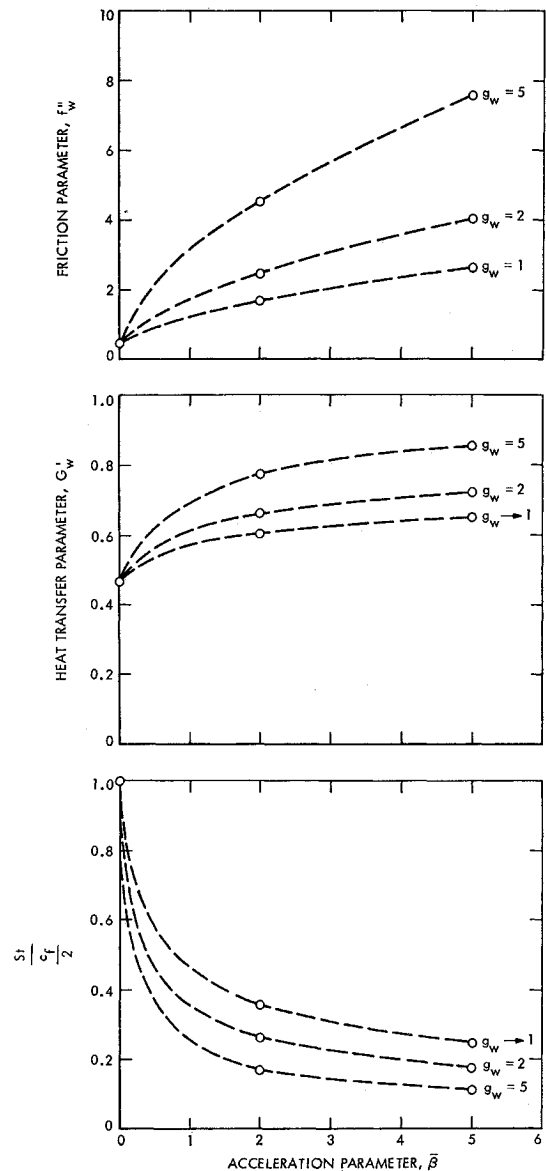


Fig. 1 Heat transfer and friction parameters and Reynolds analogy factor.

wall enthalpies  $H_w - H_{aw}$

$$\left[ \frac{q}{(H_w - H_{aw})\rho_e u_e} \right] Pr^{2/3} = \frac{1}{(Re_{\bar{x}})^{1/2}} \frac{G_w'}{(2)^{1/2}} \quad (5)$$

Values of  $H_{aw}$  might be calculated from a recovery factor  $\mathcal{R} = Pr^{1/2}$ , although differences between  $H_{aw}$  and  $H_{10}$  are not significant unless the flow speed is appreciable. The acceleration parameter  $\beta$  depends upon the shape of the channel, e.g., see Refs. 2 and 7. Flow acceleration can also occur in a channel where the cross-sectional area does not change, but instead is associated with energy transfer from the heated wall, which increases the kinetic energy of the flow.

The local similarity approach<sup>2,8</sup> has been found to agree well with more exact calculations for accelerated flows with wall cooling,<sup>9</sup> and may also be useful if the wall is heated rather than cooled. More extensive calculations would be helpful in appraising such a method.

Some differences in the heat transfer and wall friction relations from those given in Eqs. (5) and (4) might also be expected for real gases for which the viscosity dependence on temperature is usually less than linear, e.g., for the empirical relation  $\mu \propto T^\omega, \omega < 1$ . These differences depend upon the viscosity dependence on temperature, and consequently are

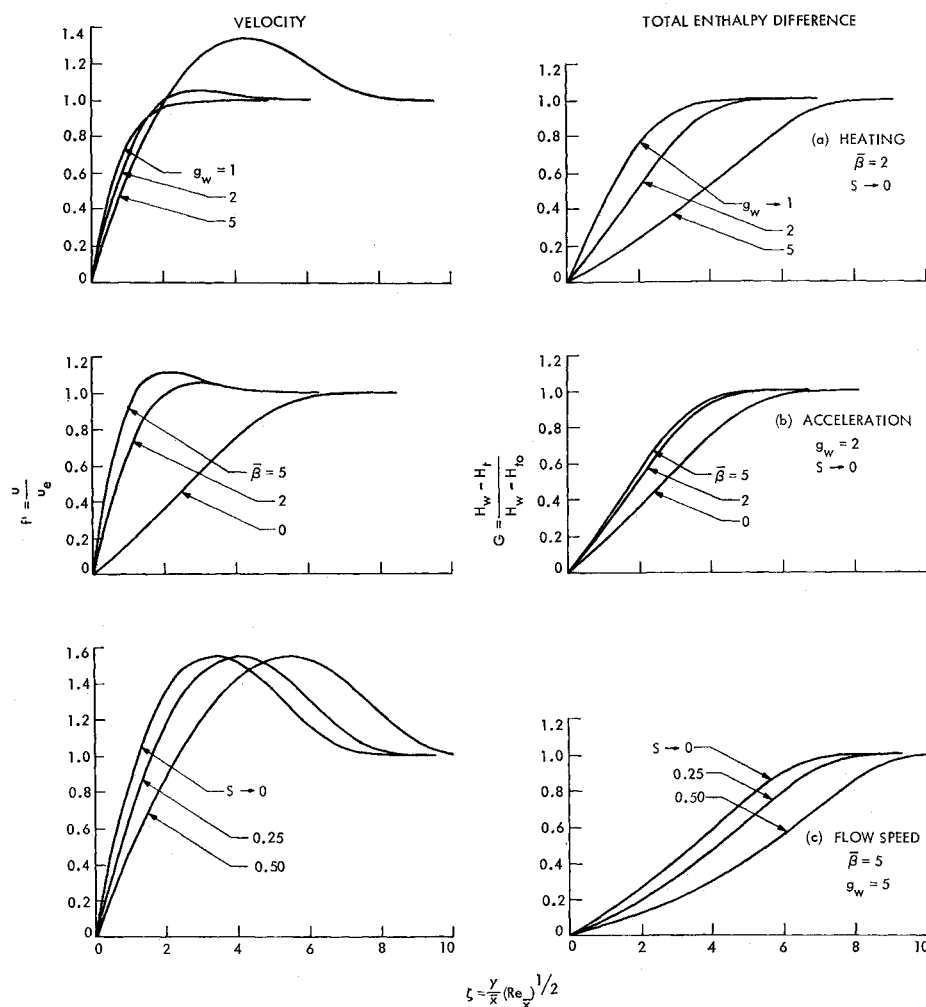


Fig. 2 Effect of wall heating, acceleration, and flow speed on the velocity and total enthalpy profiles in the physical plane.

influenced by the magnitude of  $g_w$ ,  $S$ , and  $\bar{\beta}$ . For low-speed flow ( $S \rightarrow 0$ ) with constant freestream velocity ( $\bar{\beta} = 0$ ), calculations in Ref. 3 for  $Pr = \frac{2}{3}$  indicate a rather small

change in the heat transfer and wall friction for values of  $\omega$  of 0.75 and 1.0. As an example, for a significant amount of wall heating ( $g_w = 5$ ), the predicted heat-transfer group

Table 1 Heating, acceleration and flow speed results<sup>a</sup>

Quantity	$S$	$\bar{\beta} = 0$			$\bar{\beta} = 2$			$\bar{\beta} = 5$		
		$g_w \rightarrow 1$	$g_w = 2$	$g_w = 5$	$g_w \rightarrow 1$	$g_w = 2$	$g_w = 5$	$g_w \rightarrow 1$	$g_w = 2$	$g_w = 5$
$G_w'$	Any $S$	0.4696	0.4696	0.4696	0.6052	0.6615	0.7728	0.6509	0.7204	0.8534
$f_w''$	...	0.4696	0.4696	0.4696	1.6872	2.4877	4.5236	2.6158	4.0307	7.5869
$St/c_f/2$	...	1.000	1.000	1.000	0.359	0.266	0.171	0.249	0.179	0.112
$(\theta/\bar{x})(Re_x)^{1/2}$	...	0.664	0.664	0.664	0.326	0.096	-0.598	0.224	-0.095	-1.048
$(\phi/\bar{x})(Re_x)^{1/2}$	...	0.664	0.664	0.664	0.856	0.935	1.093	0.920	1.109	1.207
$St Re_\phi$	...	0.221	0.221	0.221	0.366	0.438	0.597	0.424	0.519	0.728
$(c_f/2)Re_\theta$	...	0.221	0.221	0.221	0.389	0.169	-1.915 <sup>b</sup>	0.414	-0.270 <sup>b</sup>	-5.615 <sup>b</sup>
$(\delta^*/\bar{x})(Re_x)^{1/2} \rightarrow 0$		1.720	3.441	8.604	0.703	1.616	4.092	0.471	1.255	3.405
	0.25	2.515	4.810	11.69	1.047	2.187	5.257	0.703	1.642	4.190
	0.50	4.104	7.547	17.87	1.733	3.328	7.588	1.167	2.415	5.761
$(\delta/\bar{x})(Re_x)^{1/2} \rightarrow 0$		4.906	6.625	11.77	2.753	4.760	8.268	1.953	4.584	7.732
	0.25	5.697	7.989	14.85	3.094	5.336	9.445	2.182	4.974	8.525
	0.50	7.280	10.72	21.01	3.774	6.487	11.80	2.641	5.755	10.11
$\delta_t/\delta \rightarrow 0$		1.000	1.000	1.000	1.1510	1.089	0.957	2.042	1.071	0.951
	0.25	1.000	1.000	1.000	1.455	1.079	0.961	1.934	1.064	0.954
	0.50	1.000	1.000	1.000	1.375	1.063	0.967	1.773	1.054	0.960

<sup>a</sup> See Ref. 6 for expressions involving  $\delta$ ,  $\delta_t$ ,  $\delta^*$ ,  $\theta$ ,  $\phi$ ,  $St Re_\phi$  and  $(c_f/2)Re_\theta$  in the transformed plane. Values check the integral form of the transformed boundary-layer equations:  $\bar{\beta}(1-S)[(\delta^*/\bar{x})(Re_x)^{1/2}] = (2)^{1/2}f_w'' - [1 + \bar{\beta}(1-S)][(\theta/\bar{x})(Re_x)^{1/2}]$ ,  $(\phi/\bar{x})(Re_x)^{1/2} = (2)^{1/2}G_w'$ . With velocity overshoot,  $\delta$  is defined as the distance from the wall to the location at which  $f' = 1.01$ .

<sup>b</sup> Negative values because  $\theta$  is negative.

$St(Re_x)^{1/2}$  and friction group  $(c_f/2)(Re_x)^{1/2}$  for  $\omega = 0.75$  was less than the predicted values for  $\omega = 1$  by 12% (at  $g_w = 2$ , the difference is less, being 4–5%). The effect of flow speed (compressibility) is well known for the case of constant free-stream velocity ( $\beta = 0$ ); e.g., from Crocco's calculations (e.g., see Ref. 10) at a Mach number of 5 for  $\gamma = 1.4$  ( $S = 0.83$ ) and  $Pr = 0.725$ , values of the friction group for  $\omega = 0.75$  are below the values for  $\omega = 1.0$  by 16% for an adiabatic surface and by 10% for the highest temperature surface considered,  $g_w = 2$ . At a sonic condition  $M_e = 1$ ,  $S = 0.17$ , the respective differences are less, being lower by 1% and 5%, the latter of which is essentially the same as the low-speed value previously mentioned. Similar remarks apply to the heat-transfer group. The magnitude of these differences cited might also be found in accelerated flows by inference from recent similarity calculations in Ref. 11, which, however, were carried out for wall cooling. It would appear that differences from the values for the heat transfer and friction relations given by Eqs. (5) and (4) would be relatively small for channel flows, for example, for hydrogen and helium ( $\omega \approx 0.7$ ) at flow speeds less than sonic ( $S \leq 0.17$  and  $0.25$ , respectively).

#### IV. Concluding Remarks

The effect of large wall heating and flow acceleration on the structure of laminar boundary layers was investigated over a range of flow speeds. The heat-transfer parameter  $G_w'$  was found to increase significantly with the amount of wall heating in flow acceleration regions. This trend suggests taking advantage of heating in flow acceleration regions provided that frictional effects are not important and that the laminar boundary layer is not on the verge of transition to a turbulent boundary layer before the flow is accelerated. Because of flow acceleration the velocity profiles with wall heating do not have an inflection point in the region near the wall where the velocity increases and therefore would appear to be more stable to small disturbances. This view is supported by other observations on laminarization of turbulent flows through circular tubes,<sup>12,13</sup> where flow acceleration occurred because of energy transfer from the heated wall.

#### References

- Cohen, C. B. and Reshotko, E., "Similar Solutions for the Compressible Laminar Boundary Layer With Heat Transfer and Pressure Gradient," R-1293, 1956, NACA.
- Back, L. H. and Witte, A. B., "Prediction of Heat Transfer From Laminar Boundary Layers, With Emphasis on Large Free-Stream Velocity Gradients and Highly Cooled Walls," *Transactions of the ASME, Ser. C: Journal of Heat Transfer*, Vol. 88, Aug. 1966, pp. 249–256.
- Back, L. H., "Effects of Severe Surface Cooling and Heating on the Structure of Low-Speed, Laminar Boundary-Layer Gas Flows with Constant Free-Stream Velocity," TR 32-1301, 1968, Jet Propulsion Lab., Pasadena, Calif.
- Van Driest, E. R., "Investigation of Laminar Boundary Layer in Compressible Fluids Using the Crocco Method," TN 2597, Jan. 1952, NACA.
- Mirels, H. and Welsh, W. E., Jr., "Stagnation-Point Boundary Layer with Large Wall-to-Freestream Enthalpy Ratio," *AIAA Journal*, Vol. 6, No. 6, June 1968, pp. 1105–1111.
- Back, L. H., "Acceleration and Cooling Effects in Laminar Boundary Layers—Subsonic, Transonic and Supersonic Speeds," *AIAA Journal*, Vol. 8, No. 4, April 1970, pp. 794–802.
- Back, L. H., "Flow and Heat Transfer in Laminar Boundary Layers With Swirl," *AIAA Journal*, Vol. 7, No. 9, Sept. 1969, pp. 1781–1789.
- Lees, L., "Laminar Heat Transfer Over Blunt-Nosed Bodies at Hypersonic Flight Speeds," *Jet Propulsion*, Vol. 26, 1956, pp. 259–269.
- Marvin, J. G. and Sinclair, A. R., "Convective Heating in Regions of Large Favorable Pressure Gradient," *AIAA Journal*, Vol. 5, Nov. 1967, pp. 1940–1948.
- Howarth, L., *Modern Developments in Fluid Dynamics—High Speed Flow*, Oxford University Press, London, 1953.
- Wortman, A. and Mills, A. F., "Highly Accelerated Compressible Laminar Boundary Layer Flows with Mass Transfer," ASME Paper 70-HT/SPT-34, June 1970; *Transactions of the ASME, Ser. C: Journal of Heat Transfer*, to be published.
- Bankston, C. A., "The Transition from Turbulent to Laminar Gas Flow in a Heated Pipe," *Transactions of the ASME, Ser. C: Journal of Heat Transfer*, Vol. 92, No. 4, Nov. 1970, pp. 569–579.
- Coon, C. W. and Perkins, H. C., "Transition from the Turbulent to the Laminar Regime for Internal Convective Flow with Large Property Variations," *Transactions of the ASME, Ser. C: Journal of Heat Transfer*, Vol. 92, No. 3, Aug. 1970, pp. 506–512.

## Rotational Stability of a Semielastic Body

JOHN R. GLAESE\*

NASA George C. Marshall Space Flight Center,  
Huntsville, Ala.

IN this work we consider a system consisting of a flat plate elastically coupled to a rigid rod. This system is considered as an idealization of a rotating space station. We are interested in the effects of nonrigid coupling on the rotational stability of such systems and would like to see if there might be some advantage in using a flexible coupling between rigid parts as an aid in stabilizing a vehicle that would otherwise be unstable or in reducing the size of the control forces required and hence making a more economical system. We develop the linearized equations of motion and ascertain the stability of the linearized system as a function of the strength of the coupling for all configurations of the moments of inertia of the composite bodies. The most significant result of this work is the demonstration both mathematically and by a working model that rotation about the intermediate principal axis, which is unstable for rigid coupling, can be stabilized by weakening the coupling.

For purposes of this analysis, we assume the flat plate and rod are perfectly flat and straight, respectively, and that all motion takes place in free space. We define a body-fixed reference frame for the plate by fixing the origin at the center of mass with the  $z$  axis along the normal and  $x$  and  $y$  along the principal directions. The rod is coupled semielastically to the plate; i.e., it is joined in such a way that it can rotate in the  $x, z$  plane about the  $y$  axis and such that the equilibrium is

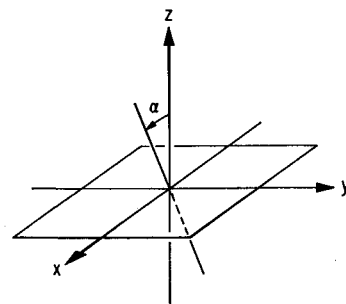


Fig. 1 Plate-fixed coordinate system.

Received November 9, 1970; revision received January 18, 1971.

\* Presently on active duty with U.S. Army Corps of Engineers, assigned to the George C. Marshall Space Flight Center, NASA, Huntsville, Ala., in the Dynamics and Control Division, Aero-Astrodynamic Laboratory.